DETERMINATION OF SEISMIC LINEAMENTS IN THE AEGEAN AREA AND DEFORMATION VELOCITIES

VLASTOS Serafeim[1,2,3]**, PAPADIMITRIOU Eleftheria**[1]**, PAPAZACHOS Constantinos**[1] **& KARAKOSTAS Vassilios**[1]

1. Geophysics Department, School of Geology, University of Thessaloniki, GR54006 Thessaloniki, Greece
2. British Geological Survey, Murchison House, West Mains Road, Edinburgh EH9 3LA, UK
3. Department of Geology and Geophysics, West Mains Road, University of Edinburgh, Edinburgh EH9 3JW, UK

Abstract

An attempt to determine the active seismic structures in the broader Aegean area is presented, in order to refine our knowledge about the active seismic faults associated with the generation of strong earthquakes. A statistical analysis aiming to define such linear structures was performed on the basis of the linear clustering of earthquakes using a complete and homogeneous catalog of instrumentally recorded earthquakes. Quality criteria, constraints and statistical tests have been proposed in order to obtain reliable results. Seismogenic regions were defined in the study area on the basis of the determined seismic lineaments and additional relevant information for the regions where the current analysis has not resulted in robust lineament determination. In each seismogenic region the seismic moment rate and the representative fault plane solution were calculated and used for the estimation of the deformation pattern. The obtained lineament orientation and spatial variation of deformation velocities contributes to our understanding on the tectonics and kinematics of the broader Aegean area.

Key words: seismic lineaments, seismic slip rates, Aegean area

1. Introduction

The Aegean region is one of the most active tectonic regions of the Alpine-Himalayan belt, with its most prominent tectonic feature the subduction of the eastern Mediterranean lithosphere under the Aegean Sea along the Hellenic Arc (Fig. 1). Papazachos and Comninakis (1970, 1971) first suggested that the subduction of the African tectonic plate under the Aegean was related to the northward motion of the African plate with respect to the Aegean and the identification of intermediate–depth earthquakes beneath the southern Aegean. Seismicity is very high throughout the arc, which is dominated by thrust faulting with a NE–SW direction of the axis of maximum compression. McKenzie (1970, 1972, 1978) showed that the northward motion of the Arabian plate pushes the smaller Anatolian plate westwards along the North Anatolian fault. This motion is transferred into the Aegean in a southwesterly direction, resulting in the northern Aegean being dominated by dextral strike–slip faulting of northeasterly strike. This faulting style is consistent with several fault plane solutions of recent strong earthquakes, as well as neotectonic observations.

The southern Aegean characterized by the presence of a belt of thrust faulting, which runs along the southwester coasts of Yugoslavia and continues south along the coastal regions of Albania and northwester Greece, and terminates north of central Ionian Islands. This type of faulting is connected with the continental collision between the External Hellenides and the Adriatic microplate. The direction of the maximum compression axis is almost normal to the direction of the Adriatico–Ionian geological zone. Between continental collision to the north and oceanic subduction to the south, in the area of central Ionian Islands, the most prominent feature of tectonic origin is the Cephalonia Transform Fault (CTF). It has been recognized as a major discontinuity between the Apulian platform and the West Hellenic Arc, first suggested by Scordilis et al. (1985) who found that the large 1983 Kefalonia earthquake (M7.0) has a dextral strike-slip mechanism, is oriented in a northeast direction and dips to the southeast. The fault follows the submarine Kefalonia valley west of the island chain from Kefalonia to Lefkada. The CTF is extended to the Lefkada fault segment along the western coast of Lefkada Island (Louvari et al., 1999).

The exact rupture lengths even for some of the most recent events as well as for most other past events cannot unambiguously defined but may only be inferred from the available information. Such cases concern faults that are mostly offshore for which there is neither observation about surface fault traces

nor reliably estimated aftershocks that could help in defining their rupture extend. A way to overcome this difficulty is to use other indirect techniques aiming to help defining the rupture zones of past events. Such techniques were applied by Papazachos et al. (1999) to spatially define the rupture zones of 150 strong (M$\geq$6.0) shallow earthquakes in the Aegean and surrounding area. The rupture zones have been investigated by field observations of surface fault traces, accurate location of spatial clusters of aftershocks or other smaller earthquakes, reliable fault plane solutions and information on the spatial distribution of sites with high (I$\geq$VIII) macroseismic intensities. The validity of these four techniques was successfully tested by comparing the results of their application to several cases of recent strong shallow earthquakes. Papazachos et al. (2001) used seismological (distribution of epicenters, macroseismic information, focal mechanisms) and geological data (surface fault traces, stratigraphy and geomorphology data) for the determination of the properties of the faults where the known major (M$\geq$6.0) shallow (h$\leq$40km) earthquakes have occurred in Greece and surrounding area since 480 BC.
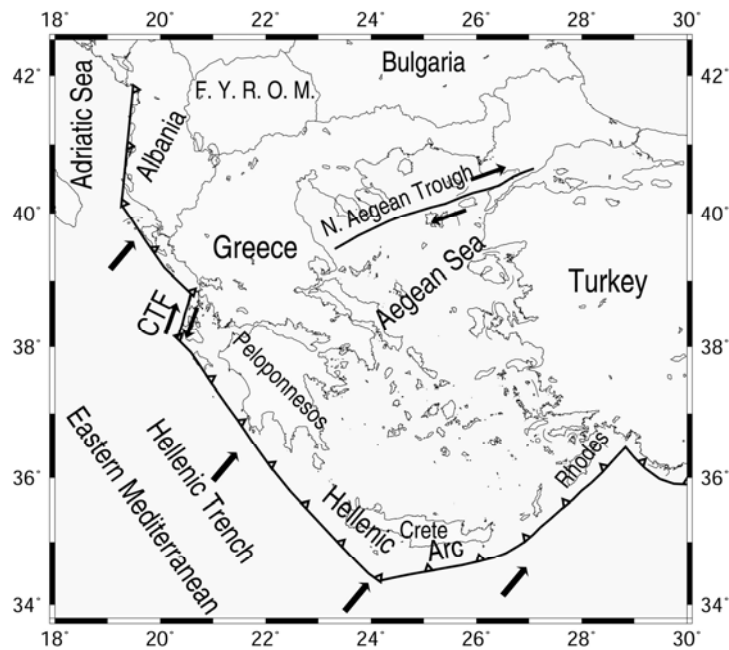

Fig. 1. *Main seismotectonic properties of the Aegean and surrounding regions.*

In this paper an alternative method applies, which is based on the statistical analysis of a complete and homogeneous catalog of earthquakes that have occurred in the broader Aegean area. According to this method, active seismic linear structures can be defined on the basis of earthquake epicenters spatial distribution. Even if surface fault traces do not follow a straight line, linear structures of the order of tens to hundreds of kilometers are the most likely candidates for active faults, which are among the very few features in nature that are really straight. The method applied in the present work was first introduced and applied by DeRubeis et al. (1991), and Tosi et al. (1994). In the present study additional constrains have been proposed and several tests were performed in order to define the seismolineaments as accurately as possible. As it will be shown below, some of the defined active structures are related with groups of faults that have failed individually. These structures were further used to define the zones that include the most important active faults of the study area, and for each zone the deformation rate was computed on the basis of the available information concerning the seismicity and fault plane solutions.

2. Determination of seismotectonic lines in the Aegean area

A map depicting the spatial distribution of seismicity can provide an idea of epicentral concentration on certain sites, even at a first glance. This depends on the scale of map configuration and

on the scale of the features we are interested in, which makes the discrimination of these special features more complicated. In the case of definition of seismic active faults capable to produce strong earthquakes a more careful inspection is needed, since seismicity is not reduced along such faults alone but it is rather distributed in broader areas. Thus, seismicity manifestation is the necessary condition but not efficient to reveal the presence, orientation and extend of such active structures. Therefore, statistical treatment and certain constrains are needed in order to exhibit which of the epicentral concentrations are really connected with active seismic faults. On the other hand, by proving that part of the results obtained by such an analysis is in good agreement with results and observations otherwise derived, one can assess if some structures that have not been found to be related with known active faults, can be considered as candidates to produce strong earthquakes in the future.

The definition of seismic lineaments and their discrimination from any random linear epicentral alignment is subject to two conditions. The first condition concerns the statistically significant linear distribution of earthquakes, while the second one the homogeneous epicentral distribution of the earthquakes along each lineament, in order to avoid cases where epicenters are distributed around one or two clusters instead of the whole lineament length. Usually a set of epicenters within a circular area of radius R is considered (Fig. 2). If the epicenters are distributed along a lineament, then this lineament should match with a diameter of the circle. On the basis of this assumption the epicentral distribution is examined relatively to any possible orientation of the circle's diameter, typically using a 5° increment. For each diameter the orientation of the epicentral distribution around the diameter is examined. The linearity of this distribution is qualified by the parameter V, which is defined by the following equation (Tosi et al., 1994):

$$V = \frac{\sum_{i=1}^{n} \left(\frac{D_i}{R}\right)^2 M_i}{\sum_{i=1}^{n} M_i} \qquad (1)$$

where n is the number of earthquakes taken into account, D_i is the distance of the i–th epicenter from the examined diameter, M_i is the magnitude of the i-th earthquake, functioning as a weight factor, and R the radius length. Examination of equation (1) clearly shows that the small epicentral distance from the diameter (strong lineament) result in small V values, with V=0 if all epicenters lie along the diameter. Hence V controls the degree of epicentral scattering around each examined diameter.
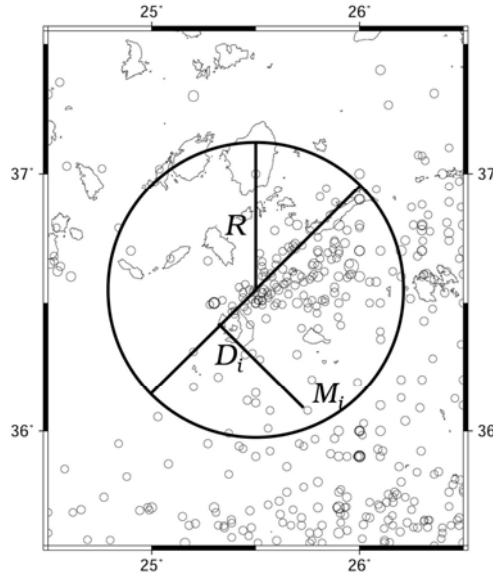

Fig. 2. *A circular area of radius R, including a certain number of earthquakes, where the analysis is performed along a certain diameter of the circle. M_i is the magnitude of an earthquake and D_i denotes the distance of its epicenter from the diameter. In each circular area 36 different orientations for the diameter were tested.*

The second condition examined concerns the homogeneity of epicentral distribution along a certain diameter. If the epicenters are normally distributed along the diameter, then a more or less uniform distribution should apply along the diameter considered. Along each segment the number n_c of the epicentral projections was calculated (weighted by the earthquake magnitude). A number of five segments is chosen so that both this number to be purposeful and a significant number of epicenters to be assigned on each segment. Testing the distribution quality is performed by the χ^2-test defined by the following equation (Tosi et al., 1994):

$$\chi^2 = \frac{\sum_{j=1}^{5}(F_{oj} - F_u)^2}{F_u} \tag{2}$$

where F_o (observed distribution) and F_u (uniform distribution) are defined as (Tosi et al., 1994):

$$F_{oj} = \sum_{k=1}^{n_c} M_k \quad \text{and} \quad F_u = \frac{\sum_{i=1}^{n} M_i}{5} \tag{3}$$

From equation (2) it is derived that the more uniform the distribution, the smaller the parameter χ^2 will be. In an absolutely uniform distribution, rarely met, the χ^2 – value becomes zero. Both parameters V and χ^2 are used in terms of probabilities and the minimum $P(V)$ and the maximum $P(\chi^2)$ values so that the derived lineaments to be reliable.

The catalogue of Papazachos et al. (2000), which provides information on earthquakes that occurred in the broader Aegean area (33°N–43°N and 18°E–30°E) for the period 550BC–1999 was used in the present study. All magnitudes reported in the catalogue are equivalent moment magnitudes (Papazachos et al., 1997; Margaris and Papazachos, 1999), with typical errors of the order of ± 0.25 for the instrumental period (1911-1999). Epicentral coordinates for the earthquakes of the period 1965-1999 have been estimated by instrumental data and their uncertainties are of the order of 20 km for the older ones (1965-1980) and 10 km for the more recent ones (1981-1999). Epicenters for the period 1901-1964 were calculated by both instrumental data and macroseismic information and their errors may reach up to 30 km.
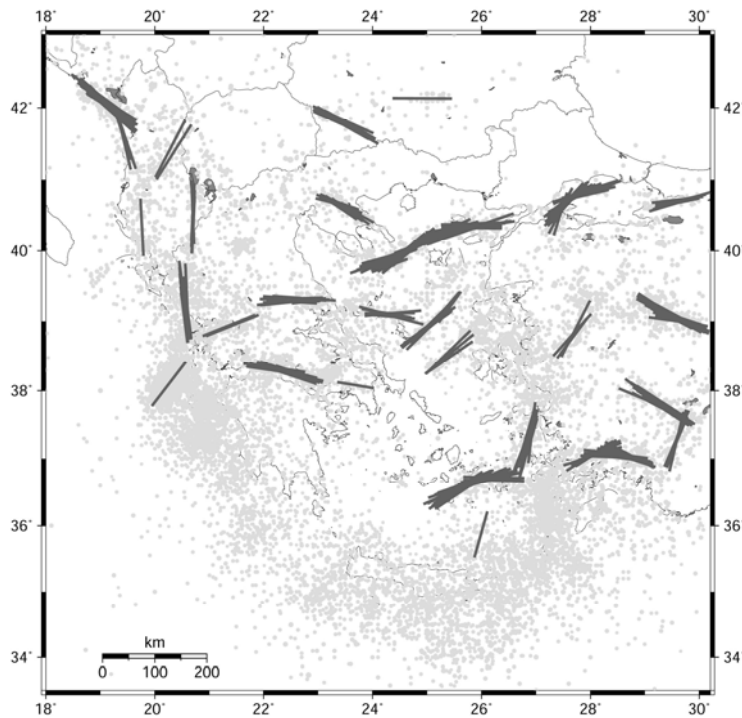

Fig. 3. *The determined lineaments together with the epicentral distribution of the earthquakes used.*

For the determination of the deformation rate in the study area it is necessary to define discrete seismogenic regions. For this purpose, in addition to the lineaments determined in the present study, the approach introduced by Papazachos and Papaioannou (1993) was taken into account. The criteria used by these authors concern the level of seismicity in each zone, the uniform distribution of seismicity and the similarity of the fault plane solutions inside each region, as well as information about accurately determined major faults in certain areas, such as the regions of Lefkada and Kefalonia. Using this approach thirty six (36) seismogenic regions were finally defined and depicted in Fig. 4 along with their code names. For each one of them deformation velocities were calculated.
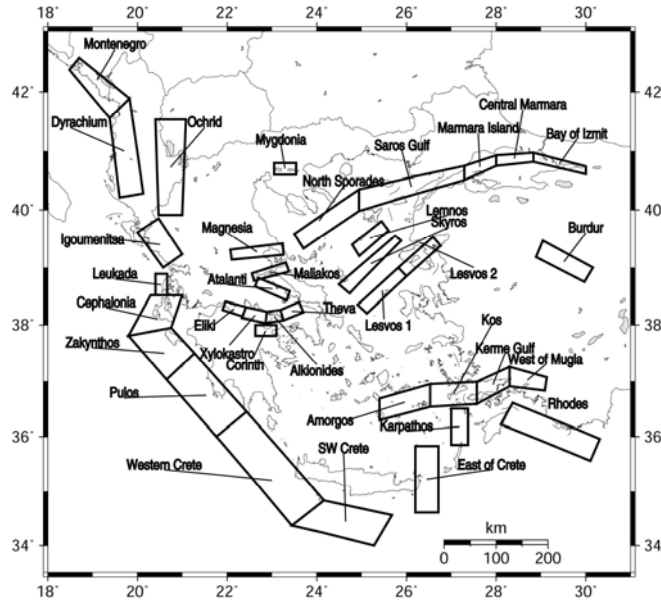

Fig. 4. *The 36 seismogenic regions examined in the present study.*

3. Seismic deformation velocities along major fracture lines

The definition of active seismogenic structures can improve significantly the estimation of active deformation in an area. Thus, the seismic lineaments previously defined in the study area constituted the basis for this calculation, in addition to the reliable fault plane solutions of strong earthquakes. The calculations were performed in 36 seismogenic regions that were defined in a way that the stress field was as much homogeneous as possible within each one of them, in order to 'encompass' all the possible sources of seismic energy release. A complete earthquake catalogue and reliable fault plane solutions were used for the calculation of the deformation rate and the 'shape' of deformation, respectively.

The original approach of Brune (1968) that refers to movements in faults that are the boundaries of tectonic plates was used after modification in the present case following Papazachos and Kiratzi (1992), since each seismogenic region is considered as a single major fault with a single fault plane solution. Such kind of movements usually leads to a kind of regional seismic activity characterized by the occurrence of earthquakes that share the same fault plane, although each one is associated with a different fault segment. The total slip caused by N earthquakes is given by:

$$\Delta U = \frac{\sum_{i=1}^{N} M_o^i}{\mu S} \qquad (4)$$

where M_o^i is the seismic moment of the i-th earthquake and S is the total area that slipped, over which ΔU is uniformly distributed. If the data set includes all the significant earthquakes during a certain time period, ΔT, and if seismicity during that period of time is representative of the activity along the boundary of the plate for greater time intervals, then the ratio $\Delta U/\Delta T$ can be assumed to be a reliable

estimate of the relative velocity of the plates (or as it is in our case of the two sides of the fault). The above approximation can apply assuming that that each side of the fault is a rigid body. The deformation rate is then calculating by the following equation:

$$\frac{\Delta U}{\Delta T} = \frac{\sum_{i=1}^{N} \dot{M_o^i}}{\mu S \Delta T} \Rightarrow \frac{\Delta U}{\Delta T} = \frac{\dot{M_o}}{\mu S} \tag{5}$$

and the area, S, of the seismic zone assuming that the fault has an oblong shape.

The seismic moment rate, $\dot{M_o}$, is given by (Molnar, 1979):

$$\dot{M_o} = \frac{A}{1-B} \cdot M_{o,max}^{(1-B)} \tag{6}$$

where $M_{o,max}$, is the seismic moment released by the maximum earthquake in the seismogenic region, having a moment magnitude equal to M_{max} and

$$A = 10^{a+(bd/c)} \quad \text{and} \quad B = \frac{b}{c}, \tag{7}$$

where a, b are the parameters of the Gutenberg–Richter (1944) relation normalized for one year, and c, d are the constants of the moment (M_o) – moment magnitude (M_w) relation.

For the slip–vector orientation in each fault area, we have used the approach of Papazachos and Kiratzi (1992, 1996) and computed for each fault area the representative focal mechanism tensor given by relation:

$$\overline{F} = \frac{\sum_{n=1}^{N} M^n}{\sum_{n=1}^{N} M_o^n} = \frac{\sum_{n=1}^{N} M_o^n F^n}{\sum_{n=1}^{N} M_o^n} \tag{8}$$

where N is the total number of the available fault plane solutions for each fault area and M^n is the corresponding moment tensor for the nth event, which can be easily decomposed as (Aki and Richards, 1980):

$$M^n = M_o^n (\overline{u} \cdot \overline{n} + \overline{n} \cdot \overline{u}) = M_o^n F^n \tag{9}$$

M_o^n is the scalar seismic moment and $\overline{u}$ and $\overline{n}$ are the unit vectors parallel to the slip vector and perpendicular to the fault plane, respectively. M_o^n essentially expresses the "size" of the deformation caused by the corresponding earthquake rupture, while tensor F^n is a "shape" tensor which expresses the "geometrical" characteristics of the corresponding deformation. It can be shown that F^n can be easily computed as a function of the azimuth, φ, the dip, δ, and the slip, λ, of the earthquake (Aki and Richards, 1980).

Tensor $\overline{F}$ is an average "shape" tensor that can be considered as a representative tensor of the typical fault plane solution of the examined area, which is supposed to be constant with time. The eigenvalues of $\overline{F}$ correspond to the mean P and T axes direction, from which the average slip-vector orientation can be easily obtained. It should be noted that equation (8) does not require that the fault-plane solution data are complete in time, hence allowing the incorporation of historical information, such as surface fault rupture, etc.

Hence the estimation of deformation velocities is performed in two–steps:
a) Seismic zones having similar tectonic characteristics (i.e. fault plane solutions) are grouped in broader zones and $\overline{F}$ is estimated for each zone using equation (8). In this case, N is the number of earthquakes that have reliable fault plane solutions in each area, allowing us to define the average orientation of the slip–vector for each zone.

b) The estimation of $\dot{M}_o$ for each zone (equation (6)) is not based on the few earthquakes with know focal mechanisms which are complete for a small period of time, as usually done when deformation velocities are estimated. On the contrary, all the available data of earthquakes (instrumental and historical) which occurred in the examined seismic zone during a much bigger period of time are used and $\dot{M}_o$ is computed using equation (6), allowing the computation of slip-rate using equation (5).

The seismic moment rate, $\dot{M}_o$, was calculated by equation (8) and the complete earthquake data sample: for M$\geq$4.0 since 1981, for M$\geq$4.3 since 1965, for M$\geq$4.5 since 1950, for M$\geq$5.0 since 1911, and for M$\geq$6.0 since 1855. The magnitude of the maximum earthquake reported in each region is taken as M_{max} in this relation, while the constants c and d of relation (7) have values of 1.5 and 15.89, respectively, for the area of Greece (Papazachos et al., 1992). The values of parameters b and a (annual value) of the Gutenberg–Richter relation for each seismogenic region were taken from a study of Papazachos (1998), Lamé's constant, μ, was set equal to $3\cdot10^{11}\,dyn\cdot cm^{-2}$ and the area, S, was calculated by multiplying the regions' length (maximum dimension of each region) and its width, estimated as $w=\dfrac{d}{sin\,\delta}$, where w is the width of the zone, d the thickness of the zone (which is equal to the depth of the seismogenic layer) and δ is the dip of the zone, as this later was determined by the representative fault plane solution. The depths of the larger (M$\geq$6.0) earthquakes that occurred in the broader Aegean region, for which reliable determination of the focal parameters exists based either on waveform inversion or recordings of local seismic networks, range from 8 to 13 km (Papazachos et al., 1998). From studies of aftershock sequences for which reliable determination of the aftershocks focal parameters also exists, it is evident that the majority of their foci are located in a seismogenic layer extending from a depth of 3 to 15km, some reaching a depth of 20km. Considering all of the above information, the thickness of the seismogenic layer in our calculations was taken equal to 12 km, in agreement with previous studies in the area (Jackson and McKenzie, 1988; Papazachos and Kiratzi, 1992, 1996).

Information on reliable fault plane solutions was not available for all the examined regions. For this reason a certain dip was assumed for each region depending on the dominant faulting pattern. For regions with thrust faulting the dip was considered equal to 33°, for the ones dominated by extension equal to 45°, and for those with strike-slip movement equal to 90°. These dips are the average values determined from the available reliable fault plane solutions and from accurate information about the properties of faults in the area of Greece (Papazachos and Papazachou, 1997). Using these dipping angles, δ, and thickness of 12 km resulted in widths of 12, 17 and 22 km for strike–slip, normal and thrust areas, respectively. Especially for the Kefalonia area, which exhibits strike–slip motion with a significant compressional component, a width of 20 km was chosen.

From the available fault plane solutions in each region, the mean tensor of the fault plane solution, $\overline{F}$, was calculated using equation (8). For three seismic zones (Corinth, Marmara Island and Lesvos 2) where no fault plane solutions were available, the representative fault plane solution (Papazachos et al., 1998) was used. It is worth to note to note here that $\overline{F}$ is the average value of the available reliable tensors F^n of the region with a weight proportional to the seismic moment M_o^n, and therefore, the larger events would affect mostly the tensor $\overline{F}$ and ultimately control the deformation. The eigenvalues of the tensor $\overline{F}$ correspond to the average axis P, T and the null-axis of the representative fault plane solution of each region. The representative fault plane solutions that resulted from the present analysis for each region (black) together with the representative fault plane solutions from the study of Papazachos et al. (1998b) (gray) for the three zones mentioned above are shown in figure 5 along with the region's code name. The results on the deformation rates (scalar velocity, azimuth and dip) for each region are presented in table 1. Velocity vectors are presented in Fig. 6, proportionally to their value and not taking into account the vector's dip.
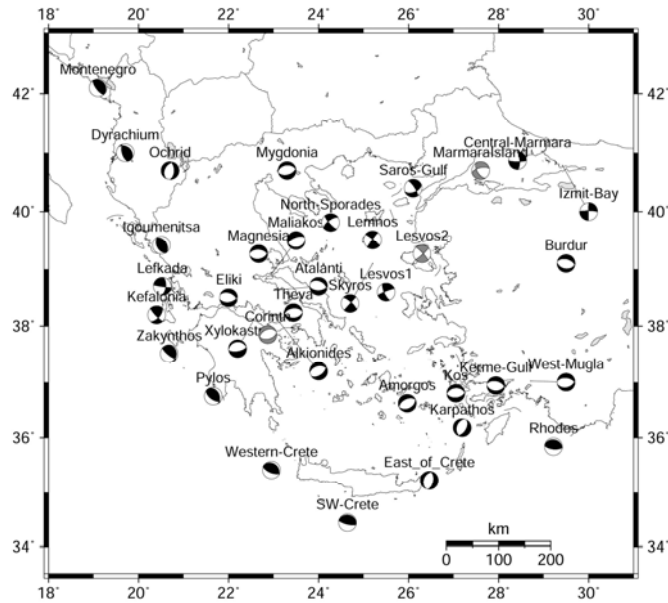
Fig. 5. *The representative fault solutions corresponding to each one of the 36 seismogenic regions examined in the present work.*
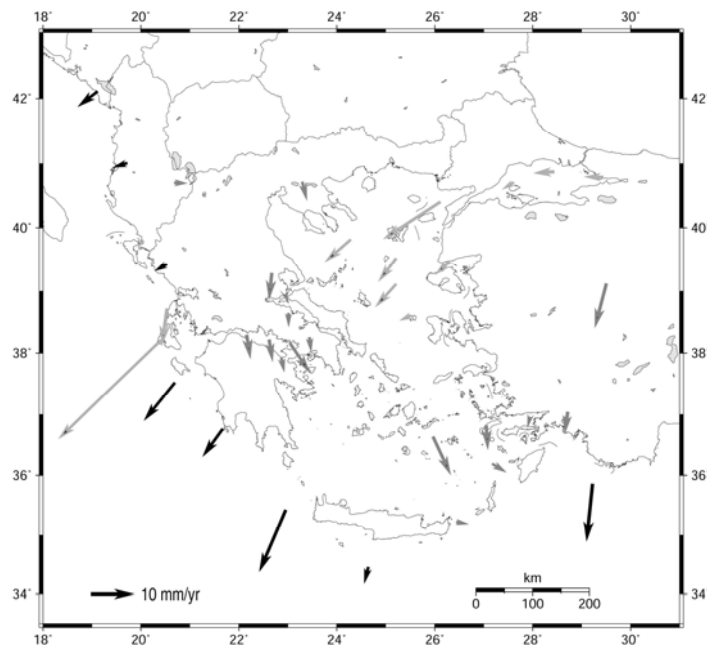

Fig. 6. *Local deformation velocities for each seismogenic region examined in the present work. The relative motion of the southernmost fault block is shown in all cases. Solid vectors correspond to thrust areas, dark–gray vectors to normal faulting areas and light–gray vectors to strike–slip faulting areas.*

5. Discussion and conclusions

An alternative method first suggested and used in the Italian territory by De Rubeis et al. (1991) was applied in the present study aiming to define the active seismic structures in the broader Aegean area by the exploitation of the spatial distribution of earthquake epicenters. To ensure the efficient application

of the method a number of criteria were set in addition to the ones set by the previously mentioned authors. After the application of the quality criteria a high population of seismic lineaments was obtained in areas of high seismicity, leading to the definition of additional criteria for the final selection of the lineaments that are adopted and presented in Fig. 3. The lineaments are in very good agreement with the known seismotectonic setting of the examined area. These lineaments describe the faulting parallel to the coasts of Albania due to the collision between the two plates. In the island of Kefalonia clear lineaments are also found, in very good agreement with the known existing transform fault in the area. In North Aegean Sea important lineaments are defined, showing the North Aegean Trough and two parallel branches to the south of it, and also clear indication of the connection to the North Anatolian fault. In central Greece they outline the faulting in Magnesia and in details the Gulf of Corinth. The lineaments found in southern Aegean and southwestern Turkey accredit the existence of a continuous active seismic zone, where a large crustal earthquake occurred during the 20th century (July 9, 1956; M7.5).

Table 1. *Information on the deformation velocities and slip vectors for the 36 seismogenic regions of the study area.*

Seismogenic region	Slip rate (mm/yr)	Slip Vector 1		Slip Vector 2	
		ξ	δ	ξ	δ
Montenegro	5.8	52	18	229	72
Dyrachium	2.9	73	28	223	59
Ochrid	2.6	272	37	116	50
Igoumenitsa	3.3	61	43	235	47
Lefkada	8.5	8	3	276	31
Kefalonia	37.4	46	10	311	30
Zakynthos	12.2	39	14	268	70
Pylos	9.2	36	31	242	56
Western Crete	18.3	23	25	216	64
SW Crete	3.2	14	16	187	74
Mygdonia	4.7	346	40	175	50
Magnesia	7.6	186	40	347	49
Maliakos	1.1	160	27	357	62
Atalanti	2.8	359	39	205	48
Eliki	6.8	351	42	201	44
Xylokastro	4.9	351	25	173	65
Alkionides	10.9	326	40	168	48
Theva	3.3	173	40	1	50
Corinth	3.3	348	41	156	48
North Sporades	8.2	49	12	144	23
Saros Gulf	17.4	237	14	338	37
Marmara Island	2.6	166	26	59	31
Central Marmara	4.3	360	10	266	19
Bay of Izmit	3.5	91	1	181	8
Lemnos	6.7	127	4	217	5
Skyros	7.4	132	0	222	14
Lesvos 1	2.1	158	7	66	17
Lesvos 2	4.4	318	7	227	8
Burdur	14.1	195	40	6	50
Amorgos	12.8	155	40	335	50
Kos	6.5	356	40	176	50
Kerme Gulf	1.8	194	40	0	49
West of Mugla	5.7	188	39	347	49
Karpathos	4.0	301	37	106	52
Rhodes	15.4	6	25	192	65
East of Crete	2.2	280	37	113	52

There are certain areas, however, where the resulting lineaments show discrepancies with the known stress field. In southwestern Bulgaria as well in the northern Greece the lineaments exhibit a NW–SE trend in contrast with the E–W trending faults associated with the generation of recent strong earthquakes. This NW–SE strike is interpreted as the predominant strike of smaller en echelon E–W trending faults. In eastern Crete and in Lefkada Island, both characterized by high seismicity the application of the method did not result in any lineament definition. This can be attributed to the high scattering of seismicity in both areas in conjunction with the very strict quality criteria applied. In a further development of the method this observation can be addressed by introducing the earthquake scattering as a decisive factor of the quality criteria. It is beyond any doubt that this method can be further developed to become a valuable tool to verify existing knowledge and to give new insight in regions where there is lack information from other sources.

It is worth to note here that the current results can contribute in outlining previously unidentified active structures in the study area. The lineament defined in Amvrakikos gulf (centered almost at 39°N–21°E) shows the continuation of the active tectonic line in Thessalia region with the ones of central Ionian Islands and western Greece, in agreement with King et al. (1993) who considered the gulf as being associated with Aegean–Ionian–European triple junction. Thus a continuation from Marmara to Ionian Sea is exhibited through Northern Aegean–Thessalia–Amvrakikos gulf. The NNE–SSW trending lineaments that are found in western Turkey and southern Aegean virtually show a continuity, although reliable fault plane solutions of recent strong earthquakes in the area are associated with almost E–W trending faults. The defined lineament direction is in agreement, however, with the conclusion of Doutsos and Kokkalas (2001) according to which NNE–SSW trending faults in this area may act as transfer faults that transmitted movements of the Anatolian plate toward the Aegean plate.

The lineaments derived by the current analysis along with information from previous investigations contributed to the division of the study area into 36 seismogenic regions where representative fault plane solutions were assigned. For each region the deformation rate and the typical slip vector were estimated, considering each region as a single major fault with a singular fault plane solution. The results were compared with previous investigations, comprising seismicity and geodetic data and were found to be in very good agreement. The map where the slip vectors area depicted (Fig. 6) provides an aggregate image on the local kinematics in the broader Aegean area. The gradual variation of the westward motion in Marmara Sea to SW motion from Northern to Southern Aegean and the similar progressive variation of the south–southwestward motion to south–southeastward motion in central Greece, as well as the consistent southwestward motion along the Hellenic Arc, are among the main characteristics that the current results outline.

References

Aki, K. & Richards, P., 1980. Quantitative Seismology: Theory and Methods. *Freeman, San Francisco, California,* pp. 557.

Brune, J., 1968. Seismic moment, seismicity, and rate of slip along major fault zones, *J. Geophys. Res.,* **73**, 777–784.

DeRubeis, V., Gasparini, C. & Tosi, P., 1991. Strutture sismogenetiche in Italia centrale. *Studi Geol. Camerti, special issue 1991/2,* 283–286.

Doutsos, T. & Kokkalas, S., 2001. Stress and deformation patterns in the Aegean region. *J. Struct. Geol.,* **23**, 455–472.

Gutenberg, B. & Richter, C. F., 1944. Frequency of earthquakes in California, *Bull. Seism. Soc. Am.,* **34**, 185–188.

Jackson, J. A. & McKenzie, D., 1988. The relationship between plate motions and seismic moment tensors, and the rates of active deformation in the Mediterranean and the Middle East. *Geophys. J. Int.,* **93**, 45–73.

King, G., Sturdy, D. & Whitney, J., 1993. Landscape geometry and active tectonics of northwest Greece, *Geol. Soc. Am. Bull.,* **105**, 137–161.

Louvari, E., Kiratzi, A. A. & Papazachos, B. C., 1999. The Cephalonia Transform Fault and its extension to western Lefkada island (Greece). *Tectonophysics,* **308**, 223–236.

Margaris, C. N. & Papazachos, C. B., 1999. Moment magnitude relations based on strong otion records in Greece. *Bull. Seism. Soc. Am.,* **89**, 442–455.

McKenzie, D. P., 1970. The plate tectonics of the Mediterranean region. *Nature*, **226**, 271–299.

McKenzie, D. P., 1972. Active tectonics of the Mediterranean region. *Geophys. J. R. astr. Soc.,* **30**, 109–185.

McKenzie, D. P., 1978. Active tectonics of the Alpine–Himalayan belt: the Aegean Sea and surrounding regions. *Geophys. J. R. astr. Soc.,* **55**, 217–254.

Molnar, P., 1979. Earthquake recurrence intervals and plate tectonics. *Bull. Seism. Soc. Am.,* **69**, 115–133.

Papazachos, B. C. & Comninakis, P. E., 1970. Geophysical features of the Greek Island Arc and Eastern Mediterranean ridge. *Com. Ren. Des Seances de la Conference Reunie a Madrid, 1969*, **16**, 74–75.

Papazachos, B. C. & Comninakis, P. E., 1971. Geophysical and tectonic features of the Aegean Arc. *J. Geophys. Res.,* **76**, 8517–8533.

Papazachos, B. C. & Papaioannou, C., 1993. Long-term earthquake prediction in the Aegean area based on a time and magnitude predictable model. *Pure Appl. Geophys.,* **140**, 593–612.

Papazachos, B. C. and Papazachou, C. B. The earthquakes of Greece. *Ziti Publications, Thessaloniki*, pp. 304, 1997.

Papazachos, B. C., Kiratzi, A. A. & Karakostas, B. G., 1997. Towards a homogeneous moment–magnitude determination for earthquakes in Greece and the surrounding area. *Bull. Seism. Soc. Am.,* **87**, 474–483.

Papazachos, B. C., Papadimitriou, E. E., Kiratzi, A. A., Papazachos, C. B. & Louvari, E. K., 1998. Fault plane solutions in the Aegean Sea and the surrounding area and their tectonic implication. *Boll. Geof. Teor. Appl.,* **39**, 199–218.

Papazachos, B. C., Papaioannou, C. A., Papazachos, C. B. & Savvaidis, A. S., 1999. Rupture zones in the Aegean region. *Tectonophysics,* **308**, 205–221.

Papazachos, B. C., Comninakis, P. E., Karakaisis, G. F., Karakostas, B. G., Papaioannou, Ch. A., Papazachos, C. B. & Scordilis, E. M., 2000. A catalogue of earthquakes in Greece and surrounding area for the period 550BC–1999. *http://geohazards.cr.usgs.gov/iaspei/europe/greece/the/catalog.htm*

Papazachos, B. C., Mountrakis, D. M., Papazachos, C. B., Tranos, M. D., Karakaisis, G. F. & Savvaidis, A. S., 2001. The faults which have caused the known major earthquakes in Greece and surrounding region between 5th century BC and today. *2nd Congress on Earthq. Engin. and Engin. Seismol., Thessaloniki, November 2001*, 17–26.

Papazachos, C. B., 1998. An alternative method for a reliable estimation of seismicity with an application in Greece and surrounding area. *Bull. Seism. Soc. Am.*, **82**, 111–119.

Papazachos, C. B. & Kiratzi, A. A., 1992. A formulation for reliable estimation of active crustal deformation and an application to central Greece. *Geophys. J. Int.,* **111**, 424–432.

Papazachos, C. B. & Kiratzi, A. A., 1996. A detailed study of the active crustal deformation in the Aegean and surrounding area. *Tectonophysics*, **253**, 129–153.

Papazachos, C. B., Kiratzi, A. A. & Papazachos, B. C., 1992. rates of active crustal defomation in the Aegean and the surrounding area. *J. Geodynamics*, **16**, 147–179.

Scordilis, E. M., Karakaisis, G. F., Karakostas, B. G., Panagiotopoulos, D. G., Comninakis, P. E. & Papazachos, B. C., 1985. Evidence for transform faulting in the Ionian Sea: The Cephalonia Island earthquake sequence. *Pure Appl. Geophys.,* **123**, 388–397.

Tosi, P., De Rubeis, V., Papadimitriou, E. & Dimitriu, P., 1994. Statistical study of epicentre alignment in the broader Aegean area. *Annali Geofisica*, **37**, 939–948.

Wessel, P. and W. H. F. Smith., 1995. New version of the Generic Mapping Tools released. *EOS, Trans. Am. Geophys. U.* **76**, 329.